Quantum Electronics **32** (9) 765–775 (2002)

INVITED PAPER

PACS numbers: 43.35.Sx; 78.20.Hp; 42.81.Dp
DOI: 10.1070/QE2002v032n09ABEH002289

Excitation of sound waves upon propagation of laser pulses in optical fibres

A.S. Biryukov, M.E. Sukharev, E.M. Dianov

***Abstract*. A revised, more comprehensive model of excitation and propagation of acoustic vibrations, electrostrictively induced in optical fibres by laser pulses, is presented. An analytic expression for the acoustic response function of the refractive index in a standard single-mode fibre is derived. Response functions are found for a standard fibre as well as for a single-mode double-clad fibre, which offers much promise for fibreoptic communication lines and where the effective area of mode-field cross section is increased with respect to a standard fibre. It is shown that the intensity of excited sound waves in double-clad fibres is usually several times higher than that in standard fibres. This intensity is determined mainly by the shape of the radial distribution of the electromagnetic field in the pulse, which is different for the fibres considered in this paper.**

Keywords: *single-mode fibre, electrostriction, sound waves, acoustic branch.*

1. Introduction

In the early 1990s, it was shown [1–4] that electrostriction is one of the physical phenomena limiting the data transmission rate in fibreoptic communication lines. This effect is known (see, e.g., [5]) to involve the deformation of dielectrics in the electric field. If the field depends on time, then the alternating deformation manifests itself as acoustic vibrations excited in a dielectric.

Fused silica fibres are typical dielectrics. Electromagnetic radiation propagating through these fibres is concentrated mainly in a comparatively narrow core, leading to a considerable spatial inhomogeneity of the field. The time-dependent radiation intensity, in the pulsed regime of propagation, in particular, determines alternating elastic stresses in a fibre. Sound waves excited due to the electrostriction give rise to spatiotemporal changes in the refractive index of glass. Even small changes in the refractive index under certain conditions should influence the propagation of optical signals through a fibre.

The first serious investigation of the electrostrictive effect in fibres was performed comparatively recently [1]. The authors of this paper proposed a model describing this effect in terms of spatiotemporal changes in the medium density caused by short pulses propagating through a single-mode fibre. In particular, this model explained the mechanism behind the previously observed effect of soliton interaction in high-repetition-rate soliton trains within large propagation lengths [6]. In papers [2–4], the model of [1] was improved and supplemented. Further investigations of acoustic effects caused by electrostriction in fibres, performed by different research groups, confirmed the basic concepts of the model approach [1]. The essence of these concepts is that the electrostrictive effect in fibres may become the most important factor limiting the high-speed transmission of large data arrays in long fibreoptic communication lines.

The most consistent description of electrostriction in fibres based on equations of the dynamic theory of elasticity was provided in [7, 8]. These studies have supplemented the results of the above-mentioned papers by showing that the influence of electrostriction on changes in the refractive index is largely determined by the polarisation of the electromagnetic field as well as by fluctuations of geometric sizes of the light-guiding structure of the fibre.

Until recently, all the investigations of electrostriction were confined to single-mode fibres with a standard light-guiding structure, where the mode field is described to a high accuracy by a Gaussian function of the radial coordinate. In the last few years, several laboratories have been conducting intense research of specific features of single-mode fibres with a different light-guiding structure, providing an increase in the effective cross-section area A_{eff} of radial mode-field distribution as compared with standard fibres. The field distribution in these fibres, which is different from the Gaussian, should also affect the electrostrictive acoustic response of fibres to radiation pulses.

One of the possible practical implementations of such a light-guiding structure is a double-clad fibre, consisting of a central solid fused silica cylinder with the cross-section radius a and the refractive index n_1, surrounded by a concentric cladding of thickness $b - a$ with the refractive index n_2, and yet another concentric glass cladding of thickness $c - b$ with the refractive index n_3. The middle cladding has the highest optical density: $n_2 > n_1, n_3$. The entire light-guiding structure is usually protected by a polymer jacket.

The aim of this paper is to analyse in detail the processes of excitation of sound waves upon propagation of laser pulses through a single-mode standard fibre and the above-described double-clad fibre. Our analysis is based on the model approach [7, 8] to the description of electrostriction

A.S. Biryukov, M.E. Sukharev, E.M. Dianov Fiber Optics Research Center, A.M. Prokhorov General Physics Institute, Russian Academy of Sciences, ul. Vavilova 38, 119991 Moscow, Russia

Received 17 May 2002
Kvantovaya Elektronika **32** (9) 765–775 (2002)
Translated by J.M. Mikhailova

in solid dielectrics. We have, however, radically revised this model.

2. Theoretical model

The choice of an adequate model is an important stage in solving the problem specified above. Electrostriction in fibres can be presently analysed using two modifications of the model, which provide different levels of approximation. Most of the papers employ the model proposed in [1]. This model can be called the hydrodynamic approximation, merely because it is based on the equation describing small fluctuations of the density ρ' of a compressible medium near the equilibrium value ρ_0. Accurate to the dissipative term in the left-hand side, this equation is a typical equation of hydroacoustics (see [9], for example):

$$\frac{\partial^2\rho'}{\partial t^2} - C^2\Delta\rho' = -\nabla \boldsymbol{F}_1, \tag{1}$$

where C is the speed of sound and $\boldsymbol{F}_1$ is the density of volume forces inducing small-amplitude acoustic vibrations in a medium. Equation (1) involves the striction force

$$\boldsymbol{F}_1 = \frac{\rho_0}{8\pi}\left(\frac{\partial\varepsilon_0}{\partial\rho}\right)\nabla E^2, \tag{2}$$

which is determined in [5] for liquid dielectrics. Here, ε_0 is the dielectric function, E is the absolute value of the vector of the electric component of the electromagnetic field.

In other words, the motion of particles in a fused silica fibre is treated in this approximation as a motion of an ideal compressible fluid.

An alternative variant of the model for the analysis of electrostriction uses the vector $\boldsymbol{U}(\boldsymbol{r}, t)$ of displacements of particles as a characteristic of the stress-deformed state of an elastic solid. In this case, acoustic vibrations of a solid are determined by solving the well-known wave equation of the linear dynamic theory of elasticity [10]:

$$\frac{\partial^2\boldsymbol{U}}{\partial t^2} + 2\Gamma\frac{\partial\boldsymbol{U}}{\partial t} - C_\mathrm{t}^2\Delta U - \left(C_\mathrm{l}^2 - C_\mathrm{t}^2\right)\mathrm{graddiv}\boldsymbol{U} = \boldsymbol{f}, \tag{3}$$

where C_l is the velocity of the sound wave where the particles oscillate along the wave vector (the longitudinal speed of sound; for fused silica, $C_\mathrm{l} = 5.996$ km s^{-1}); C_t is the velocity of the wave where particles oscillate in the direction normal to the wave vector (the transverse speed of sound; for fused silica, $C_\mathrm{t} = 3.74$ km s^{-1}); Γ is the parameter characterising the dissipation of sound; $\boldsymbol{f} = \boldsymbol{F}(\boldsymbol{r}, t)/\rho_0$; $\boldsymbol{F}$ is the vector of the density of volume forces [similar to $\boldsymbol{F}_1$ in Eqn (1)], which differs from $\boldsymbol{F}_1$ for a solid.

To clarify the physical meaning of approximations that distinguish Eqn (1) from more rigorous Eqn (3), let us transform Eqn (1) applying the continuity equation. It is easy to show that Eqn (1) is then reduced to

$$\frac{\partial^2\boldsymbol{U}}{\partial t^2} - C^2\mathrm{graddiv}\boldsymbol{U} = \boldsymbol{f}_1 = \frac{\boldsymbol{F}_1}{\rho_0}, \tag{4}$$

where C is the only speed of sound in fluid equal to C_l.

Thus, along with different expressions for $\boldsymbol{F}_1$ and $\boldsymbol{F}$ in the right-hand sides and the so far insignificant dissipative term, Eqn (1) [and equivalent Eqn (4)] differs from Eqn (3) by the absence of the term

$$C_\mathrm{t}^2(\mathrm{graddiv}\boldsymbol{U} - \Delta\boldsymbol{U}) = C_\mathrm{t}^2\mathrm{rotrot}\boldsymbol{U}. \tag{5}$$

The physical meaning of this term is explained below.

As is known, the sound field (the field of velocities $\boldsymbol{v}$ of medium elements) in an ideal fluid is potential. However, a single scalar potential function is not always sufficient to completely describe any vector field. The field has to be vortex-free, i.e., the condition $\mathrm{rot}\boldsymbol{v} = 0$ (or $\mathrm{rot}\boldsymbol{U} = 0$) should be satisfied, to make such a description complete. In an ideal liquid, the resultant of forces applied to a liquid element passes through the centre of mass of this element, giving rise to no rotational moment.

In a solid, shearing stresses appear at the boundaries of an element. As a result, each element of a solid is subject to rotating moments, becoming involved in rotational motion in addition to translations. Thus, in a solid, $\mathrm{rot}\boldsymbol{v} \neq 0$, and it is impossible to find a single scalar function that would describe the total motion.

In other words, using approximate Eqn (1) instead of Eqn (3), we assume that the motion in a solid is vortex-free and, consequently, several elastic properties related to the existence of shear deformations are neglected. The hydrodynamic character of the approximation of Eqn (1) is also due to its right-hand side, which describes a liquid dielectric. At the same time, the presence of two different velocities of perturbation propagation in solids gives rise to new effects, missing in the hydrodynamic approximation.

In this context, the model approach based on the theory of elasticity provides the most consistent description of electrostriction in optical fibres. However, papers [7, 8], which developed such a model, suffer from some inconsistencies, influencing the quantitative aspect of the results.

Before solving Eqn (3), which is a typical equation of forced vibrations, let us determine the driving force $\boldsymbol{f}$.

The density of the volume electrostrictive force $\boldsymbol{F}$ can be found from the relation [5]

$$F_i = \frac{\partial\sigma_{ik}}{\partial x_k}, \tag{6}$$

where σ_{ik} is the stress tensor, determining the change in the total momentum of the medium and the field.

If $\boldsymbol{F}$ is understood as the force acting only on the medium, then the change in the momentum per unit field volume should be subtracted from Eqn (6).

The tensor σ_{ik} for an isotropic dielectric can be represented as

$$\sigma_{ik} = \sigma_{ik}^{(0)} + \sigma_{ik}^{(\mathrm{M})} + \sigma_{ik}^{(\mathrm{str})},$$

where $\sigma_{ik}^{(0)}$ is the elastic stress tensor in the absence of the field;

$$\sigma_{ik}^{(\mathrm{M})} = \frac{\varepsilon_0}{4\pi}\left(E_iE_k - \delta_{ik}\frac{\boldsymbol{E}^2}{2}\right) + \frac{\mu_0}{4\pi}\left(H_iH_k - \delta_{ik}\frac{\boldsymbol{H}^2}{2}\right) \tag{7}$$

is the so-called Maxwellian stress tensor [5], $\boldsymbol{E}$ and $\boldsymbol{H}$ are the electric and magnetic components of the field, μ_0 is the magnetic permeability (for fused silica, $\mu_0 = 1$ with a high accuracy); δ_{ik} is the Kronecker delta;

$$\sigma_{ik}^{(\mathrm{str})} = -\frac{1}{8\pi}\left(a_1E_iE_k + a_2\delta_{ik}\boldsymbol{E}^2\right) \tag{8}$$

is the striction component of the stress tensor.

The quantities a_1 and a_2 in Eqn (8) are the coefficients determining the expansion of the dielectric tensor in terms ε_{ik} of the components of the deformation tensor S_{ik}. Due to the deformation, the initially scalar dielectric function of an isotropic solid generally becomes the second-rank tensor. If we neglect quadratic and higher order terms in S_{ik}, our expansion is reduced to [5]

$$\varepsilon_{ik} = \varepsilon_0\delta_{ik} + a_1 S_{ik} + a_2\delta_{ik}\mathrm{Sp}\hat{S}. \tag{9}$$

In case of an isotropic dielectric, the paper [11] gives expressions relating the coefficients a_1 and a_2, appearing in Eqns (8) and (9), to the elastooptic constants, known for fused silica [12], $P_{11} = 0.121$, $P_{12} = 0.27$:

$$a_1 = -\varepsilon_0^2(P_{11} - P_{12}), \quad a_2 = -\varepsilon_0^2 P_{12}\,. \tag{10}$$

Note that the expression for the striction tensor given in [7, 8] differs from Eqn (8) by the dependence of a_1 on elasto-optic constants in Eqn (10) and the opposite sign of the coefficient a_2.

Perturbations of the refractive index induced by light pulses propagating in a fibre appear against the background of elastic stresses $\sigma_{ik}^{(0)}$, which already exist in the fibre. These elastic stresses are independent of the field and will be neglected in the calculation of $\boldsymbol{F}$.

In accordance with Eqn (6), we first determine the contribution to the volume force density corresponding to the Maxwellian stress tensor (7). Using the Maxwell equations and assuming the absence of free charges and currents, we obtain

$$\boldsymbol{F}^{(\mathrm{M})} = \frac{\varepsilon_0}{4\pi c}\frac{\partial}{\partial t}[\boldsymbol{EH}] - \frac{E^2}{8\pi}\nabla\varepsilon_0, \tag{11}$$

where c is the speed of light in vacuum.

Then, applying Eqs (8) and (6) to find the force related to the striction component of the stress tensor, we derive the following expression for the total density of volume forces:

$$\boldsymbol{F} = -\frac{1}{8\pi}\left[a_1(\boldsymbol{E}\nabla)\boldsymbol{E} + a_2\nabla\boldsymbol{E}^2 + \frac{a_1}{\varepsilon_0}\boldsymbol{E}(\boldsymbol{E}\nabla)\varepsilon_0 + \left(1 + \frac{2a_2}{\varepsilon_0}\right)\boldsymbol{E}^2\nabla\varepsilon_0\right] + \frac{\varepsilon_0 - 1}{4\pi c}\frac{\partial}{\partial t}[\boldsymbol{EH}]. \tag{12}$$

In real fibres, the radial distribution of the dielectric function is such that the difference in ε_0 between the layers of the light-guiding structure does not exceed 1 % – 3 %. Calculations show that, even for large dielectric-function gradients between the layers, the smallness of absolute changes in the dielectric function makes the role of the terms in Eqn (12) involving $\nabla\varepsilon_0$ negligible. Formally, the neglect of these terms in Eqn (12) corresponds to a step approximation of the radial profile of the refractive index in a fibre with uniform dielectric functions in each layer of the light-guiding structure.

The electric and magnetic components of a transverse wave propagating in a uniform medium are related to each other by the following relation [5]:

$$\boldsymbol{H} = \varepsilon_0^{-1/2}[\boldsymbol{kE}]\,, \tag{13}$$

where $\boldsymbol{k}$ is the unit vector in the direction of wave propagation. Then, the Abraham force [the last term in Eqn (12)], which is an analogue of the recoil effect in mechanics, is given by

$$\boldsymbol{F}_{\mathrm{A}} = \frac{\varepsilon_0^{-1/2}(\varepsilon_0 - 1)}{4\pi c}\,\boldsymbol{k}\,\frac{\partial E^2}{\partial t}. \tag{14}$$

In other words, this force has a component along the fibre axis.

With above-specified approximations, Eqn (12) gives the following expressions for the components of the mass driving force $\boldsymbol{f}$ in Eqn (3) in the cylindrical system of coordinates:

$$f_r = -\frac{1}{8\pi\rho_0}\left[a_1\left(E_r\frac{\partial E_r}{\partial r} + \frac{E_\varphi}{r}\frac{\partial E_r}{\partial\varphi} + E_z\frac{\partial E_r}{\partial z} - \frac{E_\varphi^2}{r}\right) + 2a_2\left(E_r\frac{\partial E_r}{\partial r} + E_\varphi\frac{\partial E_\varphi}{\partial r} + E_z\frac{\partial E_z}{\partial z}\right)\right],$$

$$f_\varphi = -\frac{1}{8\pi\rho_0}\left[a_1\left(E_r\frac{\partial E_\varphi}{\partial r} + \frac{E_\varphi}{r}\frac{\partial E_\varphi}{\partial\varphi} + E_z\frac{\partial E_\varphi}{\partial z} + \frac{E_rE_\varphi}{r}\right) + \frac{2a_2}{r}\left(E_r\frac{\partial E_r}{\partial\varphi} + E_\varphi\frac{\partial E_\varphi}{\partial\varphi} + E_z\frac{\partial E_z}{\partial\varphi}\right)\right], \tag{15}$$

$$f_z = -\frac{1}{4\pi\rho_0}\left[\frac{a_1}{2}\left(E_r\frac{\partial E_z}{\partial r} + \frac{E_\varphi}{r}\frac{\partial E_z}{\partial\varphi} + E_z\frac{\partial E_z}{\partial z}\right) + a_2\left(E_r\frac{\partial E_r}{\partial z} + E_\varphi\frac{\partial E_\varphi}{\partial z} + E_z\frac{\partial E_z}{\partial z}\right) - \frac{\varepsilon_0^{-1/2}(\varepsilon_0 - 1)}{c}\frac{\partial E^2}{\partial t}\right],$$

where E_r, E_z and E_φ are the radial, longitudinal, and azimuthal components of the electric field, respectively.

At each instant of time, the electromagnetic field in a single-mode fibre is linearly polarised along a certain axis x of the plane Cartesian coordinate system (x, y) related to an arbitrary cross section of the fibre. At the same time, $E_x = E_0(t, z)V(r)$ and $E_y = E_z = 0$, so that

$$E_r = E_0(t,z)V(r)\cos\varphi, \quad E_\varphi = -E_0(t,z)V(r)\sin\varphi, \quad E = E_0(t,z)V(r). \tag{16}$$

In what follows, we will restrict ourselves to the consideration of light pulses with flat edges. For such pulses, the longitudinal derivative of the field intensity is much lower than the transverse one. This assumption usually holds true when the length of a comparatively smooth pulse along the z axis substantially exceeds the thickness of the fibre core [it is evident that $E_0(t, z) = E_0(t)$ in this case]. In this approximation, we can neglect with an adequate accuracy the longitudinal component of the driving force f_z as compared with the transverse components and consider the in-plane problem in an arbitrary fixed cross section of a fibre.

Under the assumptions made, substituting Eqn (16) into Eqn (15), we write down the components of the force

$$f_r = -\frac{E_0^2(t)V(r)}{16\pi\rho_0}\frac{\partial V(r)}{\partial r}(a_1 + 4a_2 + a_1\cos 2\varphi),$$
$$f_\varphi = \frac{E_0^2(t)V(r)}{16\pi\rho_0}\frac{\partial V(r)}{\partial r}a_1\sin 2\varphi. \quad (17)$$

Note that in the expressions of f_r and f_φ in [7, 8], the multiplier $V(r)/\rho_0$ is missing in addition to the above-mentioned incorrect dependence of the force components on the elastooptic constants.

Given the relation between the driving force and the pulse $[E_0(t), V(r)]$ and fibre $[a_1, a_2, \varepsilon_0(r)]$ properties, we next turn to the solving of Eqn (3). We treat a fibre as a cylinder of an infinite length with a circular cross section, where the elastic properties of different layers of the light-guiding structure are identical with a high accuracy. The velocities C_1 and C_t in polymer jacket substantially differ from those in fused silica; thus, for sound wave this fibre generally corresponds to a coaxial two-layer cylinder. The polymer jacket, as shown, in particular, in [13], plays an important role in the propagation of sound waves in a fibre, since such waves are characterised by high losses, resulting from consecutive reflections from a glass–polymer interface.

As usually, we search for the solution of the inhomogeneous equation (3) as an expansion over the complete basis of eigenfunctions of the relevant homogeneous equation.

A large number of papers is devoted to the problem of eigenfunctions and eigenvalues of a solid elastic cylinder of an infinite length, as well as to the analogous problem for a cylinder with an elastic cladding made of a different material. A detailed review and analysis of solutions of these problems can be found, e.g., in [14]. In particular, it follows from these solutions that eigenfunctions group into infinite sets (branches), which differ from each other in functional dependences on coordinates. A specific driving force excites the corresponding specific branches of acoustic vibrations. Thus, under the above-made assumptions, the motions propagating along the axis ($f_z = 0$) should not be excited. In other words, only vibrations with eigenfunctions depending exclusively on the radial and azimuthal coordinates are excited. The time dependence of each eigenfunction corresponds to a harmonic oscillation with an eigenfrequency ω_m (ω is the circular frequency, m is the number of the eigenfunction). Therefore, the solution of Eqn (3) can be obtained as

$$\boldsymbol{U}(\boldsymbol{r}, t) = \sum_m A_m(t)\boldsymbol{u}_m(\boldsymbol{r})\exp(-\mathrm{i}\omega_m t - \Gamma t), \quad (18)$$

where $\boldsymbol{u}_m(\boldsymbol{r})$ is the coordinate dependence of eigenfunctions of the homogeneous equation corresponding to Eqn (3), $A_m(t)$ are the expansion coefficients to be determined.

Considering $\boldsymbol{u}_m(\boldsymbol{r})$ to be known, we substitute Eqn (18) into Eqn (3). Then, using the orthogonality of eigenfunctions, we derive equations for $A_m(t)$:

$$\frac{\mathrm{d}^2 A_m(t)}{\mathrm{d}t^2} - 2\mathrm{i}\omega_m\frac{\mathrm{d}A_m(t)}{\mathrm{d}t} = \frac{\Phi_m}{B_m}E_0^2(t)\exp[(\mathrm{i}\omega_m + \Gamma)t], \quad (19)$$

where

$$\Phi_m = \int (\boldsymbol{g}(\boldsymbol{r}), \boldsymbol{u}_m(\boldsymbol{r}))\mathrm{d}S, \quad B_m = \int (\boldsymbol{u}_m(\boldsymbol{r}))^2\mathrm{d}S. \quad (20)$$

Here, the function $\boldsymbol{g}(\boldsymbol{r})$ is the coordinate dependence of the vector of the driving force $\boldsymbol{f}(\boldsymbol{r}, t)$ [see Eqn (17)]. The integration in Eqn (20) is performed over the area of the fibre cross section.

The general solution to Eqn (19) for an arbitrary function $E_0(t)$ is written as

$$A_m(t) = \left[C_{1m}\cos\omega_m t + C_{2m}\sin\omega_m t + \frac{\Phi_m}{\omega_m B_m} \times \int_0^t E_0^2(x)\exp(\Gamma x)\sin\omega_m(t-x)\mathrm{d}x\right]\exp(\mathrm{i}\omega_m t), \quad (21)$$

where C_{1m}, C_{2m} are the integration constants.

It is obvious that for the moments of time $t \leqslant 0$, when no electromagnetic field is applied in the considered cross section of a fibre, the sum of the first two terms in Eqn (21) is generally nonzero. Physically, this corresponds to the presence of a certain initial level of acoustic vibrations, caused by fluctuations of the fibre density at the actual temperature of the fibre. We will be interested hereinafter only in the electrostrictive contribution to the acoustic field, keeping only the last, field-dependent term in Eqn (21).

For simplicity, we also assume that the electromagnetic field is a pulse of such a duration τ that it can be approximated with a Dirac delta function, $E_0(t) = E_0\delta(t/\tau)$. The latter assumption is valid for laser pulses with lengths shorter than the minimum among the characteristic times of the acoustic response of the system $\tau_{\min}$. In the problem under study, the radius of the cross section of the fibre core a is the smallest geometric size; thus, we have $\tau_{\min} \sim a/C_1 \approx 1$ ns. Therefore, pulses with $\tau < 100 - 200$ ps can be approximated by the delta function. Under this approximation, the integral in Eqn (21) is easily taken,

$$A_m(t) = \frac{E_0^2\tau\Phi_m\exp(\mathrm{i}\omega_m t)}{\omega_m B_m}\sin\omega_m t, \quad (22)$$

and the solution (18) can be written as

$$\boldsymbol{U}(\boldsymbol{r}, t) = E_0^2\tau\exp(-\Gamma t)\sum_{m=0}^{\infty}\boldsymbol{u}_m(\boldsymbol{r})\frac{\Phi_m}{\omega_m B_m}\sin\omega_m t, \quad (23)$$

where Γ is understood in what follows as a decay caused by the losses of acoustic energy due to reflection from the glass–polymer interface. In the absence of a polymer jacket, sound waves in a fibre become long-lived [13] due to the fact that the reflection coefficients for these waves at the glass–air interface are close to unity.

Let us then specify the class of functions $\boldsymbol{u}_m(\boldsymbol{r})$ that determine the solution (23). In the general case, the eigenfunctions of a solid homogeneous cylinder with a circular cross section and infinite length can be represented as [14]

$$\boldsymbol{U}_{0m}^{(n)}(\boldsymbol{r}, t) = \left(W_m^{(n)}(r)\begin{Bmatrix}\sin n\varphi\\ \cos n\varphi\end{Bmatrix}, \Theta_m^{(n)}(r)\begin{Bmatrix}\cos n\varphi\\ -\sin n\varphi\end{Bmatrix}, Z_m^{(n)}(r)\begin{Bmatrix}\sin n\varphi\\ \cos n\varphi\end{Bmatrix}\right)\exp\left(\mathrm{i}\gamma z - \mathrm{i}\omega_m^{(n)}t - \Gamma t\right), \quad (24)$$

where $n \geqslant 0$, $m \geqslant 1$ are integer numbers, the number n determining the type of vibration symmetry and the index m numbering the roots of the characteristic equation determining the frequencies $\omega_m^{(n)}$; γ is the propagation constant, being equal to zero in our case (i.e., the absence of motions propagating along z); $W_m^{(n)}(r)$, $\Theta_m^{(n)}(r)$, $Z_m^{(n)}(r)$ are the radial dependences of the components of eigenvectors. The multipliers involving trigonometric functions in curly brackets signify that, for each pair of numbers n and m (in the case of $n \geqslant 1$), there are two equivalent eigenfunctions, which differ only by their dependences on the azimuth angle.

Since in our model approach the components of the driving force (17) contain both the terms independent of φ and the terms dependent on 2φ, of all the available normal modes (24), only the vibrational mode branches corresponding to $n = 0$ and $n = 2$ are excited. We know from the literature on acoustics that, in the absence of the longitudinal component of the displacement vector, R_{0m}, T_{0m}, and TR_{2m} could be such branches.

Axisymmetric branches R_{0m} and T_{0m}, corresponding to the condition $n = 0$ and eigenfunctions independent of the azimuth angle φ, differ in the following: in the general case, the components $W_m^{(0)}(r)$ and $Z_m^{(0)}(r)$ (in our case $Z_m^{(0)}(r) = 0$) are nonzero for the first branch, while the component $\Theta_m^{(0)}(r)$ is nonzero for the second branch. However, one can see from Eqn (17) that the component f_φ of the driving force has no terms independent of φ. Therefore, the T_{0m} branch is not excited, but only two branches of the whole set of normal modes (24) should be excited: R_{0m}, which is named the family of longitudinal normal modes, and TR_{2m} – the family of bending normal modes of a high (second) circular order. For the branch TR_{2m}, the two components of the displacement vector (24) are nonzero: namely, $u_{rm}^{(2)}(\boldsymbol{r}) = W_m^{(2)}(r)\cos 2\varphi$ and $u_{\varphi m}^{(2)}(\boldsymbol{r}) = -\Theta_m^{(2)}(r)\sin 2\varphi$ (the superscripts hereafter specify the branch, R_{0m} or TR_{2m}).

The problem of normal modes of an elastic solid cylinder is self-adjoint, and, consequently, the eigenfunctions are orthogonal to each other. The functions within each branch (with different n) are also orthogonal with respect to m; thus, the eigenfunctions form a complete basis.

The expressions for the radial dependences $W_m^{(0)}(r)$ and $W_m^{(2)}(r)$, $\Theta_m^{(2)}(r)$ of eigenfunctions for both the R_{0m} branch and the double-degenerate TR_{2m} branch can be found, e.g., in [13]. The characteristic equations for the determination of $\omega_m^{(n)}$ for both branches are also given in that paper.

Having obtained the displacement vector by the above-described method taking into account the specific form of the driving force (17), we represent the components of this vector $\boldsymbol{U}(\boldsymbol{r}, t)$ in the following way:

$$U_r(r, \varphi, t) = U_r^{(0)}(r, t) + U_r^{(2)}(r, t)\cos 2\varphi,$$
$$U_\varphi(r, \varphi, t) = U_\varphi^{(2)}(r, t)\sin 2\varphi. \tag{25}$$

Finally, we should obtain the response function, i.e., the spatiotemporal change in the refractive index. Since the refractive index is uniquely defined by the dielectric constant, we will find the function of the dielectric-constant response. For this purpose, we use the expansion (9) and the relation between the components of the vector $\boldsymbol{U}(\boldsymbol{r}, t)$ and components of the deformation tensor S_{ik}, which is known from the theory of elasticity (see [13], for example):

$$S_{rr}(r, \varphi, t) = \frac{\partial U_r(r, \varphi, t)}{\partial r},$$
$$S_{\varphi\varphi}(r, \varphi, t) = \frac{U_r(r, \varphi, t)}{r} + \frac{1}{r}\frac{\partial U_\varphi(r, \varphi, t)}{\partial \varphi},$$
$$S_{r\varphi}(r, \varphi, t) = \frac{1}{2}\left[\frac{1}{r}\frac{\partial U_r(r, \varphi, t)}{\partial \varphi} + \frac{\partial U_\varphi(r, \varphi, t)}{\partial r} - \frac{U_\varphi(r, \varphi, t)}{r}\right]. \tag{26}$$

The components of the symmetric tensor of the dielectric-function increment, caused by the electrostriction, can be determined from Eqn (9) as $\delta\varepsilon_{ik} = \varepsilon_{ik} - \varepsilon_0\delta_{ik}$, or

$$\delta\varepsilon_{rr} = (a_1 + a_2)S_{rr} + a_2 S_{\varphi\varphi},$$
$$\delta\varepsilon_{\varphi\varphi} = (a_1 + a_2)S_{\varphi\varphi} + a_2 S_{rr}, \tag{27}$$
$$\delta\varepsilon_{r\varphi} = a_1 S_{r\varphi}.$$

To find the experimentally measured maximum changes in the dielectric function, we transform the tensor $\delta\varepsilon_{ik}$ (27) to the Cartesian coordinates diagonalising this tensor averaged over the azimuth angle. Performing the necessary mathematical manipulations and taking into account Eqns (25) and (26), we obtain

$$\delta\varepsilon_{xx} = \delta\varepsilon_{R_{0m}} + \delta\varepsilon_{TR_{2m}},$$
$$\delta\varepsilon_{yy} = \delta\varepsilon_{R_{0m}} - \delta\varepsilon_{TR_{2m}}, \tag{28}$$
$$\delta\varepsilon_{xy} = \delta\varepsilon_{yx} = 0,$$

where $\delta\varepsilon_{r_{0m}}$ and $\delta\varepsilon_{TR_{2m}}$ are the individual contributions of both excited acoustic branches to $\delta\varepsilon_{ik}$, with

$$\delta\varepsilon_{R_{0m}} = \left(\frac{a_1}{2} + a_2\right)\left(\frac{\mathrm{d}U_r^{(0)}}{\mathrm{d}r} + \frac{U_r^{(0)}}{r}\right),$$
$$\delta\varepsilon_{TR_{2m}} = \frac{a_1}{4}\left[\frac{\mathrm{d}\left(U_r^{(2)} - U_\varphi^{(2)}\right)}{\mathrm{d}r} + \frac{U_r^{(2)} - U_\varphi^{(2)}}{r}\right]. \tag{29}$$

To simplify expressions (28), (29), we neglect the terms, containing multipliers $\cos 2\varphi$, $\sin 2\varphi$, $\cos 4\varphi$ and $\sin 4\varphi$, which vanish after the averaging over the cross section of the fibre. Finally, the tensor function of the response of the refractive index is given by

$$\delta n_{ik} = \frac{1}{2\varepsilon_0^{1/2}}\frac{\int \delta\varepsilon_{ik} V^2(r) r\mathrm{d}r}{\int V^2(r) r\mathrm{d}r}. \tag{30}$$

In the case of the Gaussian radial distribution of the mode field $V(r) = \exp(-r^2/2a_f^2)$, which is mostly used in practice, the quantity δn_{ik} in Eqn (30) can be easily represented in the analytical form [$a_f = (A_{\mathrm{eff}}/2\pi)^{1/2}$ is the effective radius of the mode cross section]. With the high accuracy (assuming $\omega_m \gg \Gamma$) we can take $W_m^{(0)}(r) = C_m J_1(\alpha_m r)$ as the eigenfunctions of the R_{0m} branch, where $\alpha_m = \omega_m/C_1$, C_m is an arbitrary constant, J_1 is the first-order Bessel function (see, e.g., [12]). The overlap integral in Eqn (20) can be easily calculated in the case of the Gaussian distribution:

$$\Phi_m = 2\pi C_m \int_0^a r f_r(r,t) J_1(\alpha_m r)\mathrm{d}r$$

$$= \frac{C_m(a_1+4a_2)a_f^2\alpha_m}{32\rho_0}\exp\left[-\left(\frac{\alpha_m a_f}{2}\right)^2\right]. \quad (31)$$

The quantit B_m in Eqn (20) is

$$B_m = 2\pi C_m^2 \int_0^a r J_1^2(\alpha_m r)\mathrm{d}r = \pi C_m^2 a^2$$

$$\times\left[J_0^2(\alpha_m a) - \frac{2J_0(\alpha_m a)J_1(\alpha_m a)}{\alpha_m a} + J_1^2(\alpha_m a)\right]. \quad (32)$$

Next, we use the characteristic equation, which defines the eigenfrequencies of the R_{0m} branch and which is written as [13]

$$s^2 y J_0(y) - 2J_1(y) = 0, \quad (33)$$

where $y = \alpha_m a = \omega_m a/C_l$; $s = C_l/C_t$.

By using Eqn (33), expression (32) can be transformed to the form

$$B_m = \pi C_m^2 a^2 J_0^2(\alpha_m a)\,\frac{4 + s^2(\omega_m^2 a^2/C_t^2 - 4)}{4}. \quad (34)$$

In the approximation of short (delta-like) pulses, we find $\boldsymbol{U}(\boldsymbol{r},t)$ (to be precise, the only nonzero component U_r of this vector) according to Eqn (23):

$$U_r(r,t) = \frac{E_0^2\tau\exp(-\Gamma t)(a_1+4a_2)a_f^2}{8\pi\rho_0 a^2}$$

$$\times\sum_{m=0}^{\infty}\frac{\alpha_m J_1(\alpha_m r)\exp\left[-(\alpha_m a_f/2)^2\right]\sin\omega_m t}{\omega_m J_0^2(\alpha_m a)\left[4 + s^2\left(\omega_m^2 a^2/C_t^2 - 4\right)\right]}. \quad (35)$$

Hence, according to Eqns (29), (30), we obtain

$$\delta n(t) = \frac{P_0\tau(a_1+4a_2)(a_1+2a_2)\exp(-\Gamma t)}{16\pi\varepsilon_0^{3/2}cC_l\rho_0 a^2}$$

$$\times\sum_{m=0}^{\infty}\frac{\alpha_m\exp(-\alpha_m^2 a_f^2/2)\sin\omega_m t}{J_0^2(\alpha_m a)\left[4 + s^2\left(\omega_m^2 a^2/C_t^2 - 4\right)\right]}, \quad (36)$$

where P_0 is the peak power of a pulse.

The analytic expression for the TR_{2m} branch contribution to $\delta n(t)$ can be found in a quite similar way; however, it is substantially more intricate compared to Eqn (36) and is not given here.

In the case when a very high accuracy is not necessary, the contribution of the TR_{2m} branch is negligible, and the radial distribution of the mode field is described by a Gaussian function (as it is usually the case), the simplicity of formula (36) makes it very convenient for finding $\delta n(t)$.

3. Results and discussion

The validity of a model is determined by comparing the model predictions and experimental results. For the present day, we know two experimental works [15, 16], in which the acoustic response in a standard single-mode fibre in the process of laser pulse propagation was measured. However, before we turn to the analysis of results of the calculation and the comparison between the calculated and experimental data, let us qualitatively discuss the process of the propagation of perturbations of the refractive index, which appear due to the electrostriction.

First, the R_{0m} branch is a set of acoustic vibrations with purely radial direction of the particle motion corresponding to the compression and rarefaction waves. Arisen in the core and partially reflected at the glass–polymer interface, perturbations return after a time to the fibre core as an echo. In other words, the response function should contain a number of equidistant, reducing in time echo-perturbations of the refractive index, in addition to the initial perturbation. These perturbations take place at the moments of time $t_1 \approx 21$ ns, 42 ns, 63 ns, ..., divisible by the time of the sound passing (with the velocity C_l) from the fibre axis to the surface of the glass–polymer interface and backwards. The R_{0m} branch causes no other perturbations of the refractive index. Hereafter, we consider the fibre diameter d without polymer jacket to be 125 μm.

At the same time, the TR_{2m} branch describes other motions of the medium. These motions imply complicated vibrations of medium particles in the plane of a fibre cross section, which have components both along the radial direction and perpendicular to it. Radial components (compression and rarefaction) propagate with the velocity C_l and make the contribution to the response function at the moments of time from the above-mentioned row t_1. Perturbations normal to the radial direction, propagating along it with the lower velocity C_t determine the purely shear motion. Since shear motions in a medium do not change its density, it might seem that normal components should not influence the change of the refractive index. However, as is seen for example from Eqn (27), components of the dielectric tensor depend not only on compression–rarefaction deformations, but also on deformations caused by shear tensions (specifically by torsion). This follows also from the expression (29) for $\delta\varepsilon_{TR_{2m}}$, involving the shear component U_φ of the transition vector. Therefore, the slower components determine one more set of equidistant echo signals with the consecutive centres of mass coming at $t_2 \approx 33$ ns, 67 ns, 100 ns, ..., (with the period ~ 33 ns).

The initial acoustic perturbation should have the fine structure due to the processes of compression and rarefaction in the core. The compression proceeds during the time comparable with the laser pulse duration. For typical radiuses of single-mode fibre cores $\sim 3-5$ μm the character widths of peaks of the fine structure of the initial perturbation (as well as of subsequent echoes) should be about 1–2 ns.

Note that time dependences of response functions given below correspond (except for dependences shown in Fig. 3) to the fibre core, or more precisely to the points on its axis ($r = 0$).

In the experiment of the work [15] (one of investigations [15, 16] mentioned above) 50-ps pulses of 1551-nm radiation with the pulse energy of 230 pJ, delivered by diode laser, were coupled into the fibre with the core diameter of 8.8 μm and standard outer cladding diameter of 125 μm. The pulse repetition rate was 1 MHz. For the parameter $\Gamma = 2.1\times 10^7\ \mathrm{s}^{-1}$, according to [13], the time of the virtually total decay of sound in the fibre after several (about four) reflections at the glass–polymer interface is ~ 100 ns.

Therefore, in the case of the indicated pulse repetition rate, every pulse can be considered (with respect to sound vibrations) as a very close approximation to an isolated pulse, noninteracting with sound waves excited by preceding pulses.

The response function was measured by varying the time delay between the two pulses: the exciting pulse and the probe pulse of the same laser, the polarisation of which was orthogonal to the exciting pulse polarisation and the intensity was much lower. In the Sangac interferometer, the probe pulse followed the exciting pulse and acquired a phase shift relative to the latter, depending on the time delay between pulses at the input of the interferometer. The total perturbation of the refractive index, which implies the superposition of perturbations introduced by all modes of excited acoustic vibrations, was determined by using this measurable relative phase.

Fig. 1 shows the response function $\delta n_{xx}(t)$, calculated for the above experimental conditions [15]. The radial distribution of the mode field was assumed to be Gaussian. The perturbations of the refractive index presented in paper [15] correspond only to the acoustic R_{0m} branch (the t_1 sequence). Referring to [7] and considering perturbations of the TR_{2m} branch to be small, authors give no data concerning other echo-signals. The comparison of the curve shown in Fig. 1 with the experimental curve given in [15] indicates a good agreement between the theoretically calculated and experimentally measured echo signals of the t_1 sequence with respect to their intensity and structure. The only exception is the initial perturbation, which will be discussed below. At the same time, besides the echo of t_1 and t_2 sequences one can see on the calculated curve a set of echo-signals ($t \approx 27$ ns, 48 ns, ...), which we did not mention above. This set will be discussed below as well.

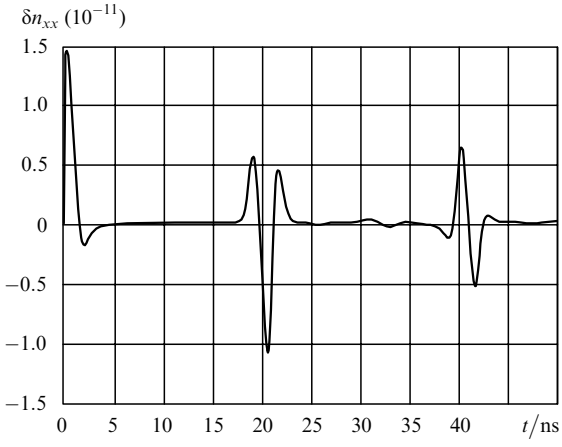

Figure 1. Acoustic response function $\delta n_{xx}(t) = \delta n_{R_{0m}}(t) + \delta n_{TR_{2m}}(t)$ calculated for the experimental conditions of [15].

In contrast to [15], in the experiment [16] optical properties of a fibre, perturbed by the intense 1547-nm exciting pulse, were probed by means of the low-power continuous laser. The 1540-nm (λ_p) radiation of this laser was coupled into a fibre of a length L simultaneously with the exciting pulse. At the fibre output the radiation of the probe laser was filtered, and then the deviation $\Delta\nu$ of the probe laser frequency from its initial value was determined by means of the Mach–Zehnder interferometer. Thus, authors of [16] measured not the response function $\delta n(t)$ (30), but the quantity

$$\Delta\nu = -\frac{L_{\text{eff}}}{\lambda_p}\frac{\partial(\delta n)}{\partial t}, \tag{37}$$

where $L_{\text{eff}} = [1 - \exp(-\alpha L)]/\alpha$; α is the optical losses in the fibre.

Works [16, 17] are remarkable because they were the first to give measured index perturbations caused by the acoustic TR_{2m} branch and to ascertain [17] that the contribution of this branch to the total electrostrictive change of the refractive index is about $\sim 20\,\%$.

The dependence $\Delta\nu(t)$, that was calculated for the experimental conditions of [16], is shown in Fig. 2. The comparison of this curve with the curve given in [16] indicates their satisfactory agreement (our results are on average twice lower than the measured ones). At that, besides the echo, forming sequences t_1 and t_2, (in particular, in the work [17]) the above-mentioned perturbations at $t \approx 27$ ns, 48 ns, ..., which were theoretically predicted by works [7, 8] and this work, can be seen both on the calculated and the experimental curve. The presence of these echo signals is concerned with physical features of the processes of the elastic wave propagation in a solid. In an infinite medium, longitudinal and shear waves propagate independently, noninteracting with each other. However, at the free boundary as well as at the media interface these waves may interact. When the purely longitudinal or purely transverse wave falls on the interface, resulting fields (of refracted and reflected waves) generally contain both waves: longitudinal and transverse. Obviously, the character of the wave does not change in the reflection for the normal incidence. It also does not change in the case of the oblique incidence of a transverse wave of such polarisation, when the transition vector is parallel to the interface. Such behaviour of elastic waves on the interface is concerned with the necessity to satisfy a number of boundary conditions, which in turn correspond to certain conservation laws. In our case, the appropriate boundary condition for Eqn (3) implies the vanishing of the components of the stress tensor.

In this work, it is impossible to go into details of this part of the theory of elasticity. We will note only the fact

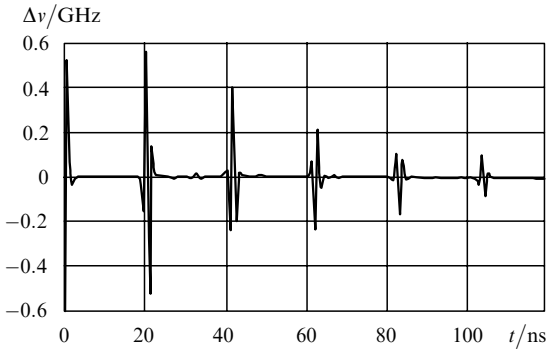

Figure 2. Electrostrictive shift of the probe laser frequency $\Delta\nu(t)$ calculated for the conditions of [16].

that the incidence of perturbation waves of the TR_{2m} branch on the glass – polymer interface is not normal. Therefore, the reflection of any of orthogonal components of that branch should be accompanied by its partial transformation into the wave of another type. The direct calculation of the radial and azimuthal components of the velocity of medium particles for the TR_{2m} branch shows that both components are nonzero in the interface, so that the resultant velocity is directed at an angle with the interface normal.

Fig. 3 most visually follows the dynamics of propagation of the perturbation in a fibre as well as that of the rise of the echo-signal of the TR_{2m} branch. Here, the calculated spatiotemporal behaviour of the function $\delta n_{TR_{2m}}(x,t) = \delta\varepsilon_{TR_{2m}}(x,t)/2\varepsilon_0^{1/2}$, averaged only over the azimuth angle φ but non-averaged over the radius, is shown in $(x,\ t)$ coordinates (the coordinate x corresponds to the radial coordinate and has different signs on the opposite sides from the axis of symmetry). One can see that each reflection on the glass–polymer interface (for $x = \pm 62.5$ μm) of either shear or longitudinal components (the inclination of their trajectories with respect to coordinate axes are different in Fig. 3) is indeed accompanied by the partial rise of the wave of a different type. This leads to the fact that a pair of echo sequences of the TR_{2m} branch, whose neighbouring centres of mass turn to be at instants $t_3 \approx (2k-1)d/(2C_l) + d/(2C_t) \approx 27$n s, 48 ns, 69 ns,... (with the same period, as that of t_1, which is about 21 ns) and at $t_4 \approx (2k+1)\times d/(2C_t) + d/(2C_l) \approx 61$ ns, 94 ns, 107 ns,... (with the same period, as that of t_2, which is about 33 ns), where k are integer numbers, arise in addition to the pair of main equidistant echo sequences (t_1 and t_2).

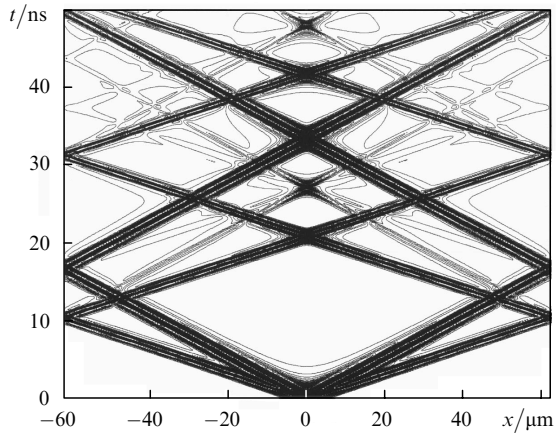

Figure 3. Component $\delta n_{TR_{2m}}(t)$ of the response function calculated for the fibre and pulse parameters given by [3].

In cited papers [7, 8, 16, 17] there are no comments concerning just described perturbations of the refractive index.

Note that the absence of the turbulent component of the motion in hydrodynamic approximation principally does not allow us to describe the acoustic response as a TR_{2m} branch. Note also that according to [7, 8] the excitation of the branch is most efficient in the case of linear electric field polarisation.

Let us say a few words about theoretical results of other authors. The comparison of our calculations with calculations of the response function made in hydrodynamic approximation [1–4] showed that our absolute values of response functions on average are twice lower than that of [4], calculated for the same parameters of the fibre and exciting laser pulse. We cannot quantitatively compare our results with the calculations made within the bounds of the model [7, 8], since the authors of those works did not give power parameters of pulses. The only result of [7, 8], which can be compared with our calculations, is the relative contribution of the acoustic TR_{2m} branch to the total response function δn. In [7, 8] this contribution is estimated as approximately 7 %. In spite of a number of inaccuracies in those works, their estimates approach values resulting from our calculations. However, both results are noticeably lower than 20 % obtained in experiment [16, 17]. The valid explanation of this fact is not found yet.

Overall, our calculations correctly describe the experimentally observed perturbations of the refractive index at the instants of time when the echo comes into the fibre core. However, it is prematurely to discuss the level of the quantitative agreement between measured and calculated response functions because of two facts. One is that calculations were performed with a number of approximations, and the other is that the authors of [15–17] give results without the experimental errors.

The first approximation of the model implies the neglect of the influence of pulse fronts on the formation and propagation of the acoustic perturbation. This approximation may adversely affect the propagation of short pulses (shorter than 10 ps). Besides this, to correctly compare the calculated results with the experiment the model should take into account the average deflections of the light-guiding structure geometry from the axisymmetric one (these deflections are always present in reality). The premature analysis testifies, for example, that the ellipticity of the core in standard two-layer fibres greatly influences the result of calculation. Depending on the scope of the core deflection from the form of a circular cylinder, the high-order TR_{qm} branches with even values of q are excited in addition to R_{0m} and TR_{2m} branches. Obviously, these additional branches will cause index perturbations, the echo signals of which will correspond exactly to above-mentioned sequences t_2, t_3, t_4. Due to this fact, the relative contribution of shear motions to the response function will be increased approaching the experimentally observed.

As for the initial perturbation of the refractive index, it implies the sum of contributions of a number of nonlinear processes determined by the third-order susceptibility. The main of them, as it was noted, e.g., in [17–21], is the quadratic Kerr effect. These processes do not directly involve the deformation of dielectric and excitation of acoustic vibrations in it, but the strictive contribution to the initial perturbation can hardly be distinguished against their background. Thus, according to the estimations of works [18, 20, 21] the Kerr-effect contribution to the nonlinear refractive index n_2 is 3–4 times greater than that of the electrostrictive effect. Remember also that in the experiment [15] the exciting pulse had the peak power of about 4.6 W, and in [17] – more than 5 W. In both cases, these values exceed the threshold of the stimulated Raman scattering (SRS). The SRS badly distorts the form of the acoustic response, measured in experiments [16, 17], for the times up to about 1 ns. By the described reasons, the papers ([16], in particular) give no initial perturbation; therefore,

the comparison of the initial perturbation measured in [15] with the calculated one is improper.

Let us analyse the results of the calculation of the response function of a single-mode double-clad fibre. Since the solving of the electrodynamic problem of the distribution of the mode field in such fibres goes beyond the scopes of our paper, let us use the data of other papers. We will give the preference to the experimentally measured distribution found by authors of [22]. This distribution is given in Fig. 4, where the radial profile of the refractive index in the fibre is schematically shown on the separate incut. Fig. 4 represents the measured distribution of the field intensity $\sim V^2(r)$, but not the field $V(r)$.

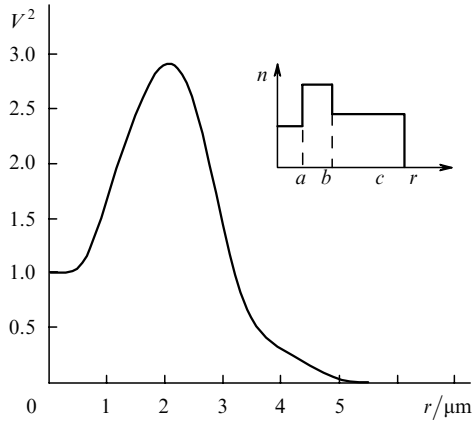

Figure 4. Normalised distribution of the intensity of the electromagnetic field of the main mode for a double-clad fibre with the high-density middle layer [22].

The quantity $A_{\text{eff}} \approx 42\ \mu\text{m}^2$ calculated for this distribution turns out to be the same order as a typical section of a mode in a standard fibre, but the distribution itself substantially differs from the Gaussian. This difference mainly lies in the following: the distribution, shown by Fig. 4, has the regions with different signs of the derivative $V'(r)$, and the form of the profile from the side of a cladding is steeper as compared with the Gaussian distribution. The rapid decay of the field in the cladding is, as a rule, achieved with the purpose to lower microbending losses. The mentioned specific features of the field distribution in a double-clad fibre determine some other form of the acoustic response functions as compared with conventional fibres considered above. This fact is illustrated by Figs 5, 6 [23], which show the contributions of R_{0m} and TR_{2m} branches calculated for a certain distribution of the field intensity (see Fig. 4) to the response function. For the comparison the response function of the standard fibre with $A_{\text{eff}} = 35\ \mu\text{m}^2$ is shown there. The calculations were made for the pulse of the duration $\tau = 50$ ns and peak power of 0.6 mW.

One can see that the response function of a double-clad fibre qualitatively keeps the same form as that of a two-layer fibre. However, both the echo and the initial perturbation acquire the more complicated structure. The more complicated fine structure of perturbations is caused by the following. In a double-clad fibre the source of perturbations is a cylindrical layer, wherein the field has its maximum, while in the case of a standard fibre perturbations arise in a narrow paraxial cylinder. As distinct from a standard fibre,

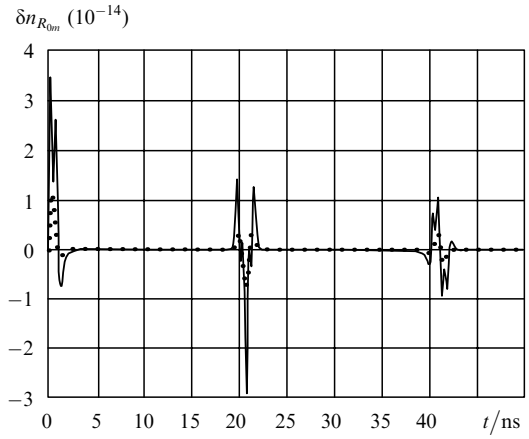

Figure 5. Contribution of the R_{0m} branch to the response function in the fibre with the ring profile of the refractive index (solid curve) and the standard two-layer fibre (dotted curve) [23].

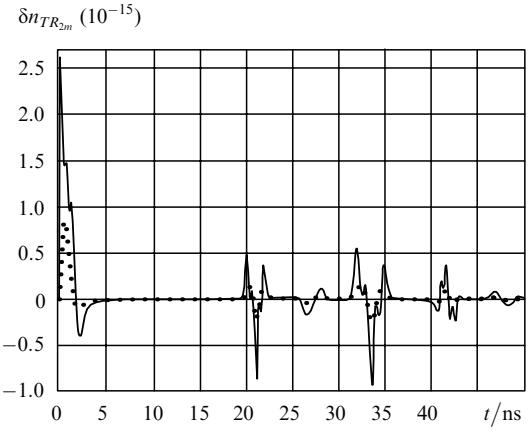

Figure 6. Same as in Fig. 5, but for the TR_{2m} branch [23].

where the duration of the initial perturbation is determined by a single character time, a double-clad fibre has at least two character times. These times are determined by two dimensions: namely, the thickness of a cylindrical layer, wherein the field has its maximum, and the radius of its cross section. As in the case of a standard fibre, the R_{0m} branch makes the main contribution to the response function, while the contribution of the TR_{2m} branch is about 4 %. We suppose also that the probability of the geometry deflection from the axial symmetry in the case of fibres with the ring profile of the refractive index is higher than that of standard fibres.

The complication of the fine structure of perturbations in a double-clad fibre is also experimentally observed. Thus, in Fig. 7, taken from the paper [24], the experimentally measured value of the frequency shift $\Delta\nu(t)$ of the probe pulse radiation (37) and the shift theoretically calculated by the above-described model, are compared. Here, the effective area of the cross section A_{eff} of the main mode is equal to 120 μm^2; therefore, the distribution of the field intensity differs from the given in Fig. 4. Both qualitative and quantitative satisfactory agreement between calculated and measured values of $\Delta\nu$ corresponding to the echo, determined by compression-rarefaction waves (the t_1 sequ-

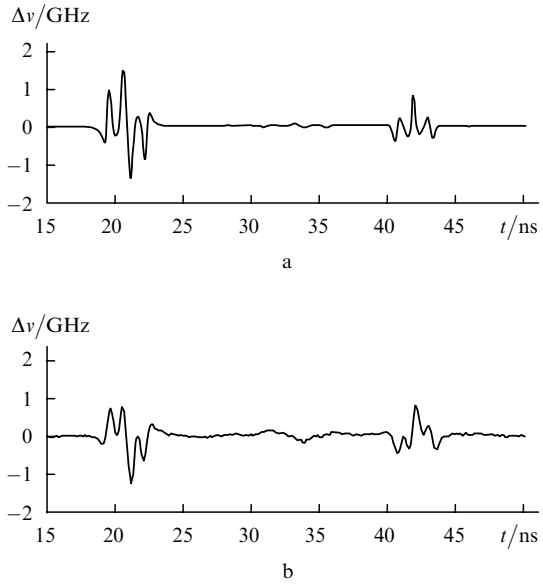

Figure 7. Comparison between the calculated (a) and the measured (b) frequency shift of the probe laser pulse radiation in the fibre with the ring light-guiding structure. $A_{\text{eff}} = 120$ μm^2, $\tau = 100$ ps, the pulse energy is 530 pJ, the fibre length $L = 9$ km, $\alpha = 0.21$ dB km^{-1} [24].

ence) is evident. Moreover, as well as in the case of standard fibres, the calculated values of Δv, corresponding to the echo related to shear motions of the medium, are lower than the measured ones.

A special attention should be paid to the fact that for the similar pulse parameters absolute values of the response function in a double-clad fibre, even for the greater value of A_{eff}, can, nevertheless, be higher than those in a standard fibre. The reason behind this fact is that the electrostrictive effect is a nonlinear phenomenon determined not by the field intensity, but by its gradient [see (17)]. The calculations confirm that for a double-clad fibre the value of $V'(r)$, exceeds the derivative of the Gaussian function by several times in a certain region of the dependence, shown in Fig. 4.

The first study of the influence of the form of the radial distribution of electromagnetic field on the electrostrictive excitation of sound in fibres was performed in [25]. By using the hydrodynamic approximation the author of this work calculated the response function in the standard fibre for the Gaussian-like function of the field intensity distribution $V^2(r) = \exp[-(r/a)^p]$ depending on the parameter p. It was found that the response function becomes smooth with the growth of p and its amplitude value decreases. However, analogous calculations performed in our work give the contrary results: the amplitude of the response function increases, while p and the value of $V'(r)$ grow. It is easy to show that the functional dependence of the δn amplitude on the p value is rising. However, starting from the certain values of p, this dependence comes to constant and then virtually does not change. Hence, the hydrodynamic approximation could lead not only to overestimated quantitative results, but also to the qualitatively different conclusions.

4. Conclusions

The model presented above allows one to calculate the function of the fibre response to the propagation of a single pulse. However, this model is far from being sufficient for the analysis of the electrostrictive effect in fibres, because from the practical point of view the investigation of the interaction of pulses in their high-frequency train, caused by the acoustic perturbation of the refractive index, is of primary importance. The relative temporal shift between pulses in the information sequence may cause considerable distortions in the process of the information transfer in fibreoptic communication lines. In this case, the electrostrictive effect can be one of the primary limitations imposed on the data transfer rate. The work [1] was the first to express this conclusion with respect to standard fibres. Later it was confirmed by a number of other investigations. The above-performed comparison between the acoustic response functions of fibres of two different types demonstrates that electrostrictive limitations of the data transfer rate even in double-clad fibres, which offer much promise for fibreoptic communication lines, would be not less (if not more) substantial. To reveal the quantitative aspect of these limitations with respect to the problem of the communication, further theoretical and experimental study of the electrostrictive effect in fibres seems to be useful.

References

1. Dianov E.M., Luchnikov A.V., Pilipetskii A.N., Starodumov A.N. *Opt. Lett.*, **15**, 314 (1990).
2. Dianov E.M., Luchnikov A.V., Pilipetskii A.N., Starodumov A.N. *Sov. Lightwave Commun.*, **1**, 37 (1991).
3. Dianov E.M., Luchnikov A.V., Pilipetskii A.N., Prokhorov A.M. *Sov. Lightwave Commun.*, **1**, 235 (1991).
4. Dianov E.M., Luchnikov A.V., Pilipetskii A.N., Prokhorov A.M. *Appl. Phys. B*, **54**, 175 (1992).
5. Landau L.D., Lifshits E.M. *Elektrodinamika sploshnykh sred* (Electrodynamics of Continuous Media) (Moscow: Nauka, 1992).
6. Smith K., Mollenauer L.F. *Opt. Lett.*, **14**, 1284 (1989).
7. Pilipetskii A.N., Luchnikov A.V., Prokhorov A.M. *Sov. Lightwave Commun.*, **3**, 29 (1993).
8. Golovchenko E.A., Pilipetskii A.N. *J. Lightwave Tech.*, **12**, 1052 (1994).
9. Shenderov E.L. *Volnovye zadachi gidroakustiki* (Wave Problems of Hydroacoustcs) (Leningrad: Sudostroenie, 1972).
10. Landau L.D., Lifshits E.M. *Teoriya uprugosti* (Theory of Elasticity) (Moscow: Nauka, 1987) p. 126.
11. Vol'kenshtein M.V. *Molekulyarnaya optika* (Molecular Optics) (Moscow: GITTL, 1951) pp 289–305.
12. Primak W., Post D.J. *Appl. Phys.*, **30**, 779 (1959).
13. Shelby R.M., Levenson M.D., Bayer P.W. *Phys. Rev. B*, **31**, 5244 (1985).
14. Thurston R.N. *J. Acoust. Soc. Am.*, **64**, 1 (1978).
15. Townsend P.D., Poustie A.J., Hardman P.J., Blow K.J. *Opt. Lett.*, **21**, 333 (1996).
16. Du Mouza L., Jaouen Y. *Proc. ECOC'97* (Edinburg, Scotland, UK, 1997) Vol. 2, p. 107.
17. Du Mouza L., Jaouen Y., Chabran C. *IEEE Photon. Techn. Lett.*, **10**, 1455 (1998).
18. Buckland E.L., Boyd R.W. *Opt. Lett.*, **21**, 1117 (1996).
19. Buckland E.L., Boyd R.W. *Opt. Lett.*, **22**, 676 (1997).
20. Fellegara A., Melloni A., Martinelli M. *Opt. Lett.*, **22**, 1615 (1997).
21. Melloni A., Frasca M., Garavaglia A., Tonini A., Martinelli M. *Opt. Lett.*, **23**, 691 (1998).

22. Liu Y., Berkey G. *Proc. ECOC'98* (Madrid, Spain, 1998) Vol. 1, p. 41.
23. Dianov E.M., Sukharev M.E., Biriukov A.S. *Techn. Digest OFC'2000* (Baltimore, Maryland, USA, 2000, ThR5) p. 264; *Opt. Lett.*, **25**, 390 (2000).
24. Jaouen Y., Dianov E.M., du Mouza L., Biriukov A.S., Sukharev M.E., et al. *Proc. ECOC'2000* (Munich, Germany, 2000) Vol. 3, p. 95.
25. Buckland E.L. *Opt. Lett.*, **24**, 872 (1999).